PHYSICAL REVIEW A **94**, 011801(R) (2016)

Glassy behavior in a one-dimensional continuous-wave erbium-doped random fiber laser

Anderson S. L. Gomes,[1,*] Bismarck C. Lima,[1] Pablo I. R. Pincheira,[1] André L. Moura,[1,2] Mathieu Gagné,[3] Ernesto P. Raposo,[4] Cid B. de Araújo,[1] and Raman Kashyap[3]

[1]*Departamento de Física, Universidade Federal de Pernambuco, 50670-901 Recife-PE, Brazil*

[2]*Grupo de Física da Matéria Condensada, Núcleo de Ciências Exatas–NCEx, Campus Arapiraca, Universidade Federal de Alagoas, 57309-005, Arapiraca-AL, Brazil*

[3]*Fabulas Laboratory, Department of Engineering Physics, Department of Electrical Engineering, Polytechnique Montreal, Montreal H3C 3A7, Canada*

[4]*Laboratório de Física Teórica e Computacional, Departamento de Física, Universidade Federal de Pernambuco, 50670-901 Recife-PE, Brazil*

(Received 5 January 2016; revised manuscript received 30 May 2016; published 25 July 2016)

The photonic analog of the paramagnetic to spin-glass phase transition in disordered magnetic systems, signaled by the phenomenon of replica symmetry breaking, has been reported using random lasers as the photonic platform. We report here a demonstration of replica symmetry breaking in a one-dimensional photonic system consisting of an erbium-doped random fiber laser operating in the continuous-wave regime. The system is based on a unique random fiber grating system which plays the role of random scattering, providing the disordered feedback mechanism. The clear transition from a photonic paramagnetic to a photonic spin-glass phase, characterized by the Parisi overlap parameter, was verified and indicates the glassy random-fiber-laser behavior.

DOI: 10.1103/PhysRevA.94.011801

A random fiber laser (RFL), which is the one-dimensional (1D) fiber waveguide version of random lasers (RLs) in bulk materials, was pioneered by de Matos *et al.* in 2007 [1], using a colloid consisting of a methanol solution of rhodamine 6G with TiO_2 particles in the core of a photonic crystal fiber. This work was followed by a demonstration of RFLs based on randomly spaced fiber Bragg gratings (FBGs) inscribed in erbium-doped fibers [2,3]. Soon after, Turitsyn and co-workers demonstrated a RFL in conventional optical fibers via Rayleigh scattering due to the refractive index fluctuations, amplified through the Raman effect [4]. Several other reports and applications of RFLs in different types of fibers followed, as reviewed in Ref. [5]. Other 1D or quasi-1D RLs have been also reported, both from the theoretical and experimental points of view [6–13]. All these accounts describe the lasing mechanism and related properties of 1D RLs, with emphasis on the threshold behavior.

RLs generally differ from conventional lasers as the feedback is provided by scattering rather than by a set of static mirrors. Such scattering can be passive, and therefore embedded in a gain medium, or active, playing a double role of scattering and gain medium. Examples of the former are colloids with laser dyes and TiO_2 particles, which were employed in the first unambiguous experimental demonstration of RLs [14], whereas the latter includes ZnO powders [15] or rare-earth-doped powders, such as neodymium, in different hosts [16,17]. Although operating mirrorless, RLs present cavity modes [18,19]. Further work on RLs is reviewed in Ref. [20], including applications and highlights of interdisciplinary results. Among these, we point out the very recent experimental demonstration of replica symmetry breaking (RSB) in RLs [21], a concept inherent to the theory of spin glasses [22] and theoretically proposed to be observed in photonic systems, particularly RLs, since 2006 [23,24].

In short, the RSB approach describes how identical systems under identical initial conditions can reach different states. By investigating the distribution of correlations between RL intensity fluctuations from pulse to pulse, the authors of Refs. [23,24] defined an analog to the Parisi overlap parameter and found evidence of a phase transition from the photonic paramagnetic to a glassy phase of light—a photonic spin-glass phase. The experimental demonstration of Ref. [21] employed a RL with functionalized thiophene-based oligomer (T_5OC_x) in amorphous solid state with planar geometry, pumped by a frequency doubled pulsed Nd:YAG laser (10 Hz, 6 ns, 1.06 μm). This 2D RL system emitted radiation with the several spikes depicting the modes riding on a broad pedestal around 610 nm when high resolution spectral measurements were employed. When a lower spectral resolution was employed, a somewhat smooth spectrum was measured. The authors analyzed the shot-to-shot intensity fluctuations to obtain the RSB signature and clearly demonstrated the photonic paramagnetic to RSB spin-glass phase transition. The theoretical and experimental works have been reviewed in Refs. [25–27]. Further observations of RSB in other RLs have followed [28,29], including the study [28,30] of its correspondence with the Lévy statistical regime of intensity fluctuations.

Here, we describe the experimental results of RSB in a 1D RL system operating in the continuous-wave (cw) regime. We employ an erbium-doped RFL (Er-RFL) in which scattering occurs from FBGs randomly spaced and prepared in a unique way such as to provide a suitable density of scatterers. Such unique type of scatter provides the basis for the system's reproducibility, as the FBGs are static.

The Er-RFL used in this work was the same device employed in Ref. [2], in which the fabrication details of FBGs can be found. For the present work, it suffices to say that a polarization maintaining Er-doped fiber was used in which a continuous grating with randomly distributed phase errors was written, instead of a random array of gratings, as in

*anderson@df.ufpe.br

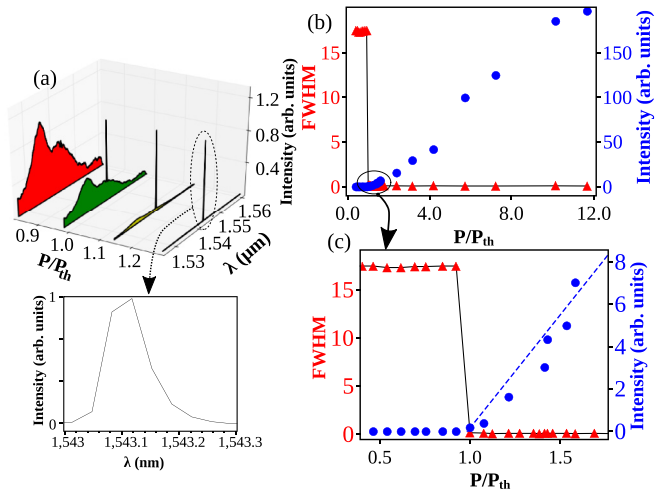

FIG. 1. (a) Spectral evolution as a function of the pump power P, normalized by the threshold power P_{th}. Detail: resolution limited lasing spectrum. (b) FWHM (triangles) and emitted intensity (circles) as a function of P/P_{th}. (c) Closer look at the threshold region in (b), showing the threshold inferred from the FWHM or output versus input intensity. Lines are guides to the eye.

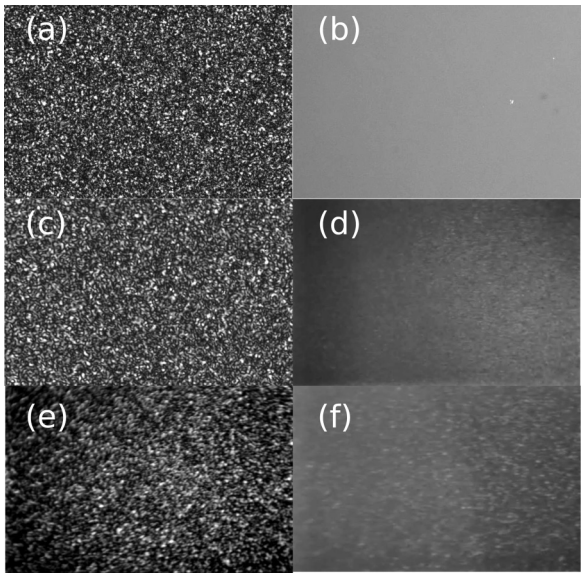

FIG. 2. Speckle images of (a) second harmonic (532 nm) of a pulsed Nd:YAG laser, (b) Rh6G-TiO_2 RL (590 nm), (c) 980 nm semiconductor laser, (d) Er-RFL pumped at 980 nm, (e) 1480 nm semiconductor laser, and (f) Er-RFL pumped at 1480 nm.

Ref. [3]. This allowed the number of scattering events and their randomness to be significantly raised. As reported in Ref. [2], Er-RFL lengths of 20 or 30 cm were used, pumped by cw laser diode pump sources operating at 980 or 1480 nm, with lasing threshold values for either Er-RFL lengths of ≈3 mW. The lengths were defined to be longer than the localization length of ≈5 cm [2]. For the results described here, the 30-cm-long Er-RFL was employed, with a cw pump source operating at 1480 nm delivering up to 200 mW power. Measurements at 980 nm pump wavelength were also performed and provided similar results.

For the statistical measurements, a sequence of 1500 spectra was collected for each pump power by directing the output of the Er-RFL onto an 86142B optical spectrum analyzer with 0.06 nm resolution, during a sweep time of 776 ms to acquire the data. Then, the power was changed and the procedure repeated. The pulse-to-pulse RFL fluctuation was not correlated to the excitation source fluctuation, as shown in Refs. [21,31].

It is important to notice that the narrowest Er-RFL spectrum measured was limited by the instrument resolution of 0.06 nm (see Fig. 1), and therefore does not show spikes representative of the longitudinal modes. Nevertheless, it has been shown in a recent work with Raman RLs [32] that, in spite of a very narrow smooth spectrum with modes averaged out [18,19], the emission is actually multimode [33]. Therefore, using the same experimental approach, we do confirm the multimode character of the RFL employed in this work (see Fig. 2 and Table I).

Figure 1 shows, for the sake of completeness, the Er-RFL characterization. The spectrum below and above the threshold for different pump powers is displayed in Fig. 1(a), while Figs. 1(b) and 1(c) show the full width at half maximum (FWHM) and emitted intensity as a function of the pump power, which was varied in steps of ≈1.0 mW from 6 to 28 mW, in steps of ≈10 mW from 28 to 38 mW, in steps of ≈20 mW from 38 to 70 mW, and in steps of ≈30 mW from 70 to 190 mW. From the data of the emitted intensity, the threshold value of 16 mW was measured, which is very different from those of Ref. [2]. This is due to the high insertion loss of some of the components used in our experimental setup. We normalize the input power P by the measured threshold P_{th}, since the studied behavior is obtained as a function of the threshold value.

In order to confirm the multimode character of the Er-RFL, the speckle contrast was measured and the number of modes was estimated [33–35]. To obtain the images of the speckle pattern a Kohler illumination system was employed [35]. To generate the phenomenon of speckle a scattering medium with dried TiO_2 (250 nm) in water solution on a microscope slide was used. The transmitted light was captured by a CCD camera operating in the visible (400–900 nm) or in the near infrared (0.4–1.9 μm). The speckle contrast is defined as [33,34]

$$C = \frac{\sigma}{\langle I \rangle} = \frac{1}{\sqrt{m}}, \tag{1}$$

where σ and $\langle I \rangle$ are the standard deviation and mean of the speckle intensity, respectively, and m is the number of lasing

TABLE I. Contrast ratio C and number of modes m for pump lasers and RLs. The Er-RFL system pumped at 980 and 1480 nm displays, respectively, $m = 236$ and $m = 204$ longitudinal modes.

Laser wavelength	Contrast and number of modes
Pump laser @ 532 nm	$C = 0.71$, $m = 2$
Pump laser @ 980 nm	$C = 0.54$, $m = 3$
Pump laser @ 1480 nm	$C = 0.70$, $m = 2$
Rh6G+TiO_2 RL @ 590 nm	$C = 0.058$, $m = 297$
1D Er-RFL @ 1540 nm	$C = 0.065$, $m = 236$
1D Er-RFL @ 1540 nm	$C = 0.070$, $m = 204$

modes. The relation between the lasing modes and the speckle contrast was recently analyzed in the context of the steady-state *ab initio* laser theory (SALT) [36–38].

The speckle contrast was measured from the central portion of the speckle pattern with an area of 600 × 600 pixels, to avoid optical aberrations produced at the edges of the sensor. This area was divided into subareas of 80 × 80 pixels, obtaining the contrast for each subdivision and averaging these results. The system was tested with a 632.8 nm cw helium-neon laser, yielding a contrast of $C = 0.81$, equivalent to ≈ 2 modes.

Figure 2 shows the speckle contrast data. For the sake of completeness and validation of the experimental setup, we measured a well-characterized RL based on a rhodamine 6G dye and 250 nm TiO_2 particles, pumped by the second harmonic (532 nm) of a pulsed (7 ns, 5 Hz) Nd:YAG laser. Figures 2(a) and 2(b) show speckle images similar to those of Ref. [35], confirming the speckle free regime for the RL. Figures 2(c)–2(f) display the results for the 30-cm-long RFL pumped either at 980 or 1480 nm. The same behavior is observed in the visible dye colloidal RL. Table I summarizes the contrast ratio and number of modes for the evaluated RLs, according to Eq. (1). Therefore, it is clearly shown that the Er-RFL operates in a multimode regime, a requirement for observation of RSB, since it relies on mode interactions.

The characterization of the RSB phase transition from the photonic paramagnetic to the spin-glass RL behavior can be quantified by an overlap parameter $q_{\gamma\beta}$ analog to the Parisi overlap parameter in spin-glass theory [22]. Two-point correlations can be calculated either among mode amplitudes a_j [24–26] or intensities $I_j \propto |a_j|^2$ [21,27], though the latter are most accessible experimentally. By measuring fluctuations in the intensity averaged over N_s system replicas, the overlap parameter reads [21,27]

$$q_{\gamma\beta} = \frac{\sum_k \Delta_\gamma(k)\Delta_\beta(k)}{\sqrt{\sum_k \Delta_\gamma^2(k)}\sqrt{\sum_k \Delta_\beta^2(k)}}, \qquad (2)$$

where $\gamma,\beta = 1,2,\ldots,N_s$, with $N_s = 1000$ for each pump power, denote the replica labels, the average intensity at the wavelength indexed by k reads $\bar{I}(k) = \sum_{\gamma=1}^{N_s} I_\gamma(k)/N_s$, and the intensity fluctuation is given by $\Delta_\gamma(k) = I_\gamma(k) - \bar{I}(k)$. In the present context, with a cw laser as the pump source, each set of emission spectrum collected within the time frame of 776 ms is considered a replica, i.e., a copy of the RL system under fairly identical experimental conditions. In this sense, we also remark that the random FBGs, which play the role of the random scattering elements, are static, thus reinforcing the replica characterization of this 1D Er-RFL system. In order to confirm that the cw measurements were appropriate, we repeated the experiment and, instead of keeping the laser on all the time, we employed a chopper before the Er-RFL system to turn the pump beam on and off at 200 Hz. The results were readily reproduced, assuring that the statistical behavior was maintained. The probability density function (PDF) $P(q)$, analog to the Parisi order parameter in RSB spin-glass theory [22], describes the distribution of replica overlaps $q = q_{\gamma\beta}$, signaling a photonic uncorrelated paramagnetic or a RSB spin-glass phase if it peaks exclusively at $q = 0$ (no RSB) or also at values $|q| \neq 0$ (RSB), respectively.

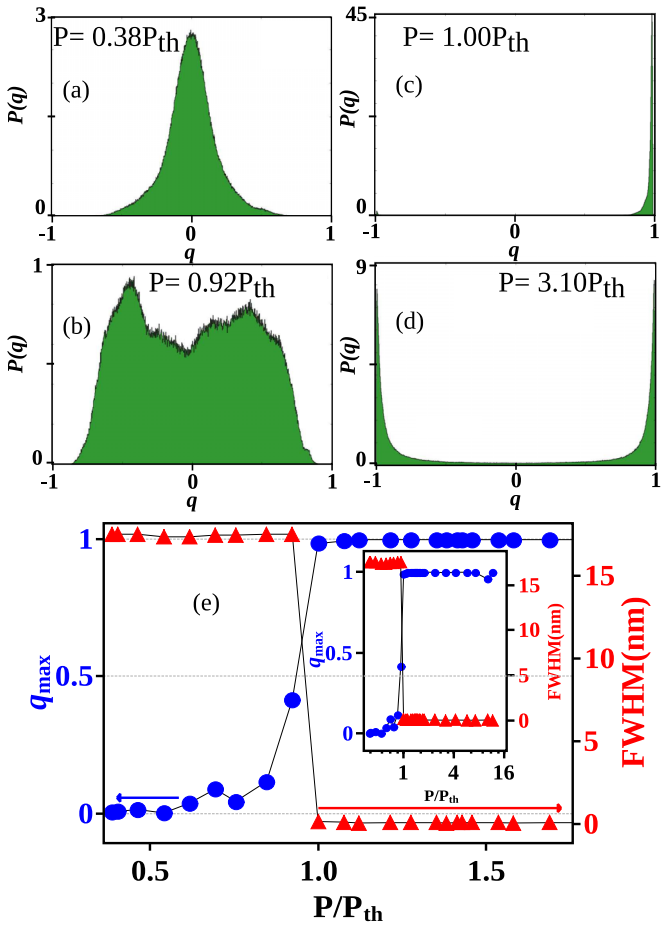

FIG. 3. (a)–(d) PDF $P(q)$ obtained from experimental data at the indicated pump powers (normalized with respect to P_{th}). (e) Value $|q| = q_{\max}$ at which $P(q)$ assumes the maximum (circles) as a function of the normalized pump power, together with the FWHM (triangles) for the sake of comparison. The inset shows the results for pump powers up to $12P_{\text{th}}$, showing the steady behavior.

Figures 3(a)–3(d) display the PDF $P(q)$ obtained from the experimental data, and Fig. 3(e) shows the value $|q| = q_{\max}$ at which $P(q)$ assumes the maximum, which is linked to the Edwards-Anderson parameter in spin-glass theory [22]. Both results are in quite good agreement with the theoretical predictions and experimental results of Ref. [21]. A sharp transition coinciding with the threshold is observed from the photonic paramagnetic [Figs. 3(a) and 3(b), below P_{th}] to the spin-glass phase with RSB [Fig. 3(d), above P_{th}]. Figure 3(e) displays $q_{\max}$ for pump powers below and above P_{th} (up to $2P_{\text{th}}$), together with the linewidth reduction for the sake of comparison. The inset shows the results for pump powers up to $12P_{\text{th}}$, showing the steady behavior.

The theoretical background that accounts for the present findings can be described as follows. In a series of remarkable works [23–27] a phase diagram for multimode RLs with disordered nonlinear medium has been recently built based on Langevin equations for the complex amplitudes of the normal modes $a_j(t)$. For open cavity systems, the general effective Hamiltonian [26,27] includes a sum of quadratic and quartic disorder terms in the mode amplitudes. The physical origin of the quadratic coupling lies in the spatially inhomogeneous

refractive index, as well as in a nonuniform distribution of the gain and an effective damping contribution due to the cavity leakage. On the other hand, the quartic coupling is related to a modulation of the nonlinear $\chi^{(3)}$ susceptibility with a random spatial profile. Such ingredients are also present in the 1D Er-RFL system analyzed in this work.

As the spatial disorder generally makes the explicit calculation of the quadratic and quartic couplings rather difficult, they have been considered in Refs. [23–27] as quenched Gaussian variables. The resulting photonic Hamiltonian for open-cavity systems thus becomes an analog to that of the spherical p-spin model [39], with a sum of $p = 2$ and $p = 4$ terms and Gaussian couplings. We remark that, in contrast with Refs. [23,24] in which the intensities were considered as essentially frozen and the relevant variables for the dynamics were solely the phases of the modes, in Refs. [25,26] the mode intensities actually took part in the dynamics on the same grounds as the phases, providing a direct link between the measurements of the overlap of intensity fluctuations and the RSB theory. In this sense, a replica-trick approach identified a phase diagram for the pumping rate as a function of the disorder strength, displaying the presence, e.g., of photonic paramagnetic, ferromagnetic, and RSB spin-glass phases, depending on the trend of the disorder to hamper the synchronous oscillation of the modes [23–27].

In the herein described 1D Er-RFL system, a higher resolution spectral measurement confirms its multimode character, in which the disorder is due to the continuous FBG in which a random distribution of phase errors was written, instead of the presence of random scattering particles [2]. Regarding the space dimensionality, we notice that the mentioned theoretical approach also works in 1D. Actually, by taking the random couplings as Gaussian variables in the photonic Hamiltonian of Refs. [23–27], the explicit connection with the spatial structure of the disordered nonlinear medium is lost, and conceivable theoretical extensions to include other sources of disorder are actually made possible. This reasoning is reinforced by the fact that, while the summations in the magnetic p-spin Hamiltonian run over the spins positions in the lattice (which necessarily take into account the explicit geometrical structure), the sums in the photonic Hamiltonian are over the mode labels, which keep no structural link with the background medium.

In conclusion, we have demonstrated an observation of RSB in a 1D RL, namely, an Er-doped RFL. The signature depicted by the Parisi parameter clearly identifies the photonic paramagnetic and spin-glass regimes, confirming the role of the RL modes as analogs to disordered spins in spin glasses. The multimode behavior was confirmed by speckle contrast measurements. Our 1D results show that this transition undoubtedly coincides with the RL threshold, confirming previous results [21,28,29]. The evidence of RSB in the cw regime also opens up important possibilities for new experimental demonstrations of other expected transitions and photonic behaviors, theoretically analyzed in Refs. [23–27].

We acknowledge the financial support from the Brazilian Agencies: Conselho Nacional de Desenvolvimento Científico e Tecnológico (CNPq) and Fundação de Amparo à Ciência e Tecnologia do Estado de Pernambuco (FACEPE). The work was performed in the framework of the National Institute of Photonics (INCT de Fotônica) and PRONEX-CNPq/FACEPE projects. A.L.M. acknowledges CNPq for support through a postdoctoral fellowship. R.K. acknowledges support from the Canada Research Chairs program of the Government of Canada.

[1] C. J. S. de Matos, L. de S. Menezes, A. M. Brito-Silva, M. A. Martinez Gámez, A. S. L. Gomes, and C. B. de Araújo, Phys. Rev. Lett. **99**, 153903 (2007).

[2] M. Gagné and R. Kashyap, Opt. Express **17**, 19067 (2009).

[3] N. Lizárraga, N. P. Puente, E. I. Chaikina, T. A. Leskova, and E. R. Méndez, Opt. Express **17**, 395 (2009).

[4] S. K. Turitsyn, S. A. Babin, A. E. El-Taher, P. Harper, D. V. Churkin, S. I. Kablukov, J. D. Ania-Castanon, V. Karalekas, and E. V. Podivilov, Nat. Photonics **4**, 231 (2010).

[5] D. V. Churkin, S. Sugavanam, I. D. Vatnik, Z. Wang, E. V. Podivilov, S. A. Babin, Y. Rao, and S. K. Turitsyn, Adv. Opt. Photonics **7**, 516 (2015).

[6] A. L. Burin, M. A. Ratner, H. Cao, and S. H. Chang, Phys. Rev. Lett. **88**, 093904 (2002).

[7] V. Milner and A. Z. Genack, Phys. Rev. Lett. **94**, 073901 (2005).

[8] F. A. Pinheiro and L. C. Sampaio, Phys. Rev. A **73**, 013826 (2006).

[9] X. Wu, J. Andreasen, H. Cao, and A. Yamilov, J. Opt. Soc. Am. B **24**, A26 (2007).

[10] A. G. Ardakani, M. Golshani, S. M. Mahdavi, and A. R. Bahrampour, Opt. Laser Technol. **44**, 969 (2012).

[11] A. K. Tiwari and S. Mujumdar, Phys. Rev. Lett. **111**, 233903 (2013).

[12] M. Gagné and R. Kashyap, Opt. Lett. **39**, 2755 (2014).

[13] A. Bahrampour, E. Shojaie, and M. Sani, J. Opt. Soc. Am. B **31**, 1308 (2014).

[14] N. M. Lawandy, R. M. Balachandran, A. S. L. Gomes, and E. Sauvain, Nature (London) **368**, 436 (1994).

[15] H. Cao, Y. G. Zhao, S. T. Ho, E. W. Seelig, Q. H. Wang, and R. P. H. Chang, Phys. Rev. Lett. **82**, 2278 (1999).

[16] A. L. Moura, V. Jerez, L. J. Q. Maia, A. S. L. Gomes, and C. B. de Araújo, Sci. Rep. **5**, 13816 (2015).

[17] M. A. Noginov, *Solid-State Random Lasers* (Springer, Berlin, 2005).

[18] H. E. Türeci, L. Ge, S. Rotter, and A. D. Stone, Science **320**, 643 (2008).

[19] J. Andreasen, A. A. Asatryan, L. C. Botten, M. A. Byrne, H. Cao, L. Ge, L. Labonté, P. Sebbah, A. D. Stone, H. E. Türeci, and C. Vanneste, Adv. Opt. Photonics **3**, 88 (2011).

[20] F. Luan, B. B. Gu, A. S. L. Gomes, K. T. Yong, S. C. Wen, and P. N. Prasad, Nano Today **10**, 168 (2015).

[21] N. Ghofraniha, I. Viola, F. Di Maria, G. Barbarella, G. Gigli, L. Leuzzi, and C. Conti, Nat. Commun. **6**, 6058 (2015).

[22] M. Mézard, G. Parisi, and M. A. Virasoro, *Spin Glass Theory and Beyond* (World Scientific, Singapore, 1987).
[23] L. Angelani, C. Conti, G. Ruocco, and F. Zamponi, Phys. Rev. B **74**, 104207 (2006).
[24] L. Angelani, C. Conti, G. Ruocco, and F. Zamponi, Phys. Rev. Lett. **96**, 065702 (2006).
[25] F. Antenucci, C. Conti, A. Crisanti, and L. Leuzzi, Phys. Rev. Lett. **114**, 043901 (2015).
[26] F. Antenucci, A. Crisanti, and L. Leuzzi, Phys. Rev. A **91**, 053816 (2015).
[27] F. Antenucci, A. Crisanti, and L. Leuzzi, Sci. Rep. **5**, 16792 (2015).
[28] A. S. L. Gomes, E. P. Raposo, A. L. Moura, S. I. Fewo, P. I. R. Pincheira, V. Jerez, L. J. Q. Maia, and C. B. de Araújo, Sci. Rep. **6**, 27987 (2016).
[29] P. I. R. Pincheira, A. F. Silva, S. J. M. Carreño, A. L. Moura, S. I. Fewo, E. P. Raposo, A. S. L. Gomes, and C. B. de Araújo, Opt. Lett. **41**, 3459 (2016).
[30] E. P. Raposo and A. S. L. Gomes, Phys. Rev. A **91**, 043827 (2015).
[31] G. Zhu, L. Gu, and M. A. Noginov, Phys. Rev. A **85**, 043801 (2012).
[32] B. H. Hokr, J. N. Bixler, M. T. Cone, J. D. Mason, H. T. Beier, G. D. Noojin, G. I. Petrov, L. A. Golovan, R. J. Thomas, B. A. Rockwell, and V. V. Yakovlev, Nat. Commun. **5**, 4356 (2014).
[33] B. H. Hokr, A. Cerjan, J. V. Thompson, L. Yuan, S. F. Liew, J. N. Bixler, G. D. Noojin, R. J. Thomas, H. Cao, A. D. Stone, B. A. Rockwell, M. O. Scully, and V. V. Yakovlev, SPIE Proc. **9731**, 973110 (2016).
[34] J. W. Goodman, *Speckle Phenomena in Optics: Theory and Applications* (Roberts & Company, Englewood, 2007).
[35] B. Redding, M. A. Choma, and H. Cao, Nat. Photonics **6**, 355 (2012).
[36] H. E. Tureci, A. D. Stone, and B. Collier, Phys. Rev. A **74**, 043822 (2006).
[37] L. Ge, Y. D. Chong, and A. D. Stone, Phys. Rev. A **82**, 063824 (2010).
[38] A. Cerjan, Y. Chong, L. Ge, and A. D. Stone, Opt. Express **20**, 474 (2012).
[39] A. Crisanti and H.-J. Sommers, Z. Phys. B **87**, 341 (1992).